Computers, Materials & Continua

Tech Science Press

https://doi.org/10.32604/cmc.2026.084783

ARTICLE

A Communication-Aware Clustered Framework for Demand Response Management in 5G-Enabled Smart Grids

Sajjad Rabbani[1], **Rao Muhammad Asif**[1], **Heba G. Mohamed**[2], **Adnan Yousaf**[1,*] **and Ateeq Ur Rehman**[3,*]

[1]Department of Electrical Engineering, Superior University, Lahore, Pakistan
[2]Department of Electrical Engineering, College of Engineering, Princess Nourah bint Abdulrahman University, Riyadh, Saudi Arabia
[3]School of Computing, Gachon University, Seongnam-si, Republic of Korea

*Corresponding Authors: Adnan Yousaf. Email: adnan.yousaf@superior.edu.pk; Ateeq Ur Rehman. Email: 202411144@gachon.ac.kr

Received: 29 April 2026; Accepted: 21 July 2026; Published: 15 September 2026

ABSTRACT: The management of demand response (DR) in smart grids increasingly relies on low-latency, reliable, and scalable communication, yet traditional DR signaling methods fail in dense network environments. In this paper, a communication-aware clustered demand response architecture (CCA-DR) for smart grids based on 5G technology is proposed, in which DR users are clustered based on service-area density and assigned to the closest communication-aware cluster. It is linked via directional antenna pairs to reduce cumulative signal attenuation. The model incorporates the properties of the 5G broadband channels, such as path loss, interference, latency, and reliability constraints, into the DR management process. A mechanism of iterative refinement is also used to enhance the cluster structure and communication quality as the load on the cells increases. The proposed framework is compared with four benchmark schemes: Distance-Only clustering, Greedy Antenna selection, Static Clustering, and Unicast DR. The simulation results indicate that the proposed CCA-DR outperforms all baselines across key communication and operational indicators. The proposed approach maintains the lowest average latency, approximately 5–13 ms across normalized cell loads from ρ = 0.1 to ρ = 1.0, remaining below the 20 ms real-time DR threshold. It also achieves lower packet loss, higher SINR, improved user rate, stronger active DR user ratio, better reliability, and stronger fairness than the benchmark schemes. The method also supports the highest user rate, the largest active user ratio of DR (around 0.95), and the best communication reliability. The framework also attains high-quality fairness of DR allocation and high-quality cell-edge SINR. Further sensitivity analysis indicates that stronger incentives lead to greater aggregate DR response in the proposed architecture. The addition of 5G communication awareness to clustering, user assignment, and antenna assignment enhances the effectiveness, resilience, and scalability of DR management in next-generation smart grids.

KEYWORDS: Demand response; communication-aware clustered demand response framework; signal-to-interference noise ratio; 5G

1 Introduction

Smart Grids (SGs) [1] are cyber-physical systems that combine advanced smart grid technologies with communication systems. They enable efficient, sustainable electricity generation and management through bidirectional communication, allowing the exchange of electricity and information across energy grids and consumer devices. This approach helps shift electricity consumption away from peak periods, resulting in a more balanced demand [2]. In SGs, utility sectors such as demand response (DR) rely on large-scale data collection from end users to forecast loads. Smart meters send real-time data, helping utilities calculate demand based on current pricing. The DR engine then responds to consumer behavior and optimizes energy use. For long-term smart-grid communication, advanced broadband and wireless connectivity are essential because they support reliable data exchange, monitoring, control, interoperability, and secure grid operation [3]. 5G emphasizes the advantages of small wireless cells and mmWave directionality, such as interference reduction and increased spatial multiplexing [4]. Moreover, multicast wireless transmission using OFDMA radio resources is emerging as an efficient means for providing group communication, particularly for massive data exchange in DR programs [5]. Advanced multimedia broadcast and multicast service (eMBMS) systems are being investigated to optimize wireless communication between aggregators and energy consumers, as well as wireless communication networks. The emerging 5G wireless broadband networks, utilizing mmWave spectrum and sub-millisecond latency, promise to meet increasing connectivity and data rate demands. Evaluations of scheduling and resource management in OFDMA systems, like those in [6], are crucial for efficient 5G deployment. Since dense small-cell deployment is foundational to 5G networks, effective planning involves selecting optimal locations for small cells equipped with directional antennas to minimize the number of small cells while providing coverage [7,8]. DR operations management generally involves (i) forecasting [9], (ii) triggering and dispatch of events, (iii) measuring and verifying, (iv) settling incentives [10], and (v) learning after events. In addition, it provides low-latency, high-reliability communications, supports an extremely high number of devices, and enables network slicing to balance grid operational priorities with communication quality-of-service (QoS). A recent dynamically priced study on DR uses multi-agent federated reinforcement learning to coordinate demand-side operations. DR management in a distributed wireless network should explicitly account for latency disparities to enhance DR transmission and responsiveness [11]. This trend indicates the operational necessity of shifting towards operational scheduling and adaptive DR, in which control policies vary with current system conditions. The communication delays and packet loss are major issues. Edge computing is once again mentioned as a viable tool to reduce DR decision latency by placing analytics and control closer to devices [12]. More recent edge-based smart grid data security research also reduces response time, a key factor in a practical DR system [13]. DR operations management should involve cybersecurity KPIs (attack detection time, trust scoring, secure key management overhead) in the performance assessment [14]. DR for industrial and commercial loads is increasingly important because large-scale flexible units require communication-enabled coordinated optimization to support grid flexibility while satisfying operational constraints and comfort margins [15]. AI assists in DR work by forecasting loads, estimating baselines, segmenting customers, predicting events, and running adaptive dispatches [16]. The main motivation for the proposed CCA-DR framework is that demand response in dense smart-grid environments cannot rely solely on energy-side scheduling or conventional communication models. In practical 5G-enabled smart grids, DR signals must be delivered under strict latency, reliability, SINR, packet-loss, and coverage constraints. Existing DR approaches mainly focus on pricing, user participation, load reduction, or energy optimization, while many 5G communication algorithms focus on handover, scheduling, or general QoS without considering DR activation. Therefore, these methods do not fully explain how communication quality affects the number of users that can be reliably activated for DR. The proposed CCA-DR algorithm differs from existing methods by jointly combining communication-aware clustering, directional antenna assignment, SINR-based link evaluation, latency-aware DR activation, and iterative cluster refinement.

The following outlines the main contributions of this article:

- A CCA-DR framework is proposed for 5G-enabled smart grids, grouping DR users by spatial distribution and communication conditions to improve scalable DR signalling.
- A joint clustering and directional antenna assignment mechanism is developed by incorporating path loss, interference, SINR, latency, reliability, and attenuation into the DR communication process.

- An iterative refinement algorithm is introduced to update the cluster structure and improve performance under dense, varying cell-load conditions, with evaluation against Distance-Only clustering, Greedy Antenna selection, Static Clustering, and Unicast DR benchmarks.

2 System Model

The proposed optimization model is formed to optimize user clustering, centroid location, antenna placement, communication quality, and DR activation. To minimize computational complexity in dense smart-grid settings, an iterative decomposition-based algorithm is proposed. The algorithm switches between communication-aware clustering, channel-based antenna selection, performance analysis, and DR response update until convergence. The simulation parameters are given in Table 1 and the other details of the proposed framework are given in following subsection.

Table 1: Simulation parameters used for evaluating the proposed 5G-enabled DR framework.

Symbol	Typical Value	Symbol	Typical Value
N, K, A	500, 9, 2×2 km^2	q_{min}	0.50
L_{max}	20	P_i, max	0.5–3 kW
d_0	1 m	$\pi_i(t)$	0.1–0.5 p.u.
PL_0, σ	32.4, 6 dB	δ_i	0.1–0.8 p.u.
n	3.1	ε_i, c(t)	0–0.2 p.u.
P_k, tx	30 dBm	$\bar{\varepsilon}_r$, $\bar{\varepsilon}_n$, $\bar{\varepsilon}_c$	0 p.u for all
h_t, h_r	10, 1.5 m	$\chi^{2\alpha}$	0.95
G_i, rx	2 dBi	ρ_{max}	180
θ_3, ϕ_3 dB	65, 15 degree	N_k,min, N_k,max	30, 80
A_{max}	20 dB	$\varepsilon\mu$, εJ	10^{-3} m, 10^{-4}
M_k	4	NMC	100 runs
N_0	−174 dBm/Hz	ω_1, ω_2, ω_3	0.40, 0.35, 0.25
B_{max}, B_i	100 MHz, 0.180–1 MHz	α_1, α_2, α_3	0.20, 0.15, 0.15
Γgap	1.5	α_4, α_5, α_6	0.10, 0.30, 0.10
Lpkt	256 bits	β_0, β_1, β_2, β_3, β_4	−1.0, 1.2, 0.20, 0.08, 1.0
τ_i,queue, τ_i,proc, τ_i,prop	2, 1, 0.5 ms	$\Lambda\tau$, τ_{max}	0.05 ms^{-1}, 20 ms
τ_i,MEC-normal, τ_i,MEC-fail	2, 8 ms	a_1, b_1	1, 0.12
$Pr\{\zeta_i = 1\}$	0.05	γ_{min}, γedge	5, 0 dB

2.1 Initialization Stage

Assume that N DR-enabled users are distributed across the service area with known coordinates $\mathrm{r}_i = [x_i, y_i]^T$, $i = 1, \ldots, N$. Let the number of clusters be K, and let $\mu_k^{(0)}$ defines the initial centroid of cluster k. These initial centroids are chosen randomly or by using a centroid seeding method such as k-means++. In the start, the variables are initialized, $\ell = 0$, $\mu_k^{(0)}$, $k = 1, \ldots, K$, $J^{(0)} = +\infty$, and $x_{ik}^{(0)} = 0$, $y_{ikm}^{(0)} = 0$, $u_i^{(0)} = 0$, where ℓ is the iteration index and $J^{(\ell)}$ is the objective function value at iteration ℓ.

2.2 Communication-Aware User Clustering

At iteration ℓ, the euclidean distance between user i and centroid k is computed in Eq. (1). The clustering cost is formulated by considering spatial distance, estimated channel loss, and an edge-quality penalty for each user in Eq. (2). Then the user assignment is performed on the cluster with the minimum cost in Eq. (3)

and the binary allocation variable is formulated in Eq. (4). This step creates the current user-to-cluster association matrix, and to prevent unbalanced cells, the cluster sizes are determined in Eq. (5). If a cluster exceeds its upper bound, its users are reassigned to neighboring feasible clusters according to the next minimum-cost assignment.

$$d_{ik}^{(\ell)} = \| \mathrm{r}_i - \mu_k^{(\ell)} \|_2 \tag{1}$$

$$\mathcal{C}_{ik}^{(\ell)} = \omega_1 \left(d_{ik}^{(\ell)}\right)^2 + \omega_2 \ell_{ik}^{\mathrm{ch},(\ell)} + \omega_3 \mathcal{P}_{ik}^{\mathrm{edge},(\ell)} \tag{2}$$

$$k_i^{*(\ell)} = \arg\min_{k \in \mathcal{K}} \mathcal{C}_{ik}^{(\ell)} \tag{3}$$

$$x_{ik}^{(\ell+1)} = \begin{cases} 1, & k = k_i^{*(\ell)} \\ 0, & \text{otherwise} \end{cases} \tag{4}$$

$$N_k^{\min} \le \sum_{i=1}^{N} x_{ik}^{(\ell+1)} \le N_k^{\max} \tag{5}$$

2.3 Channel Estimation and Directional Antenna Assignment

The path loss is computed in Eq. (6). The received power for user i from antenna pair m is calculated in Eq. (7). For each user, the best directional antenna pair is chosen in Eq. (8). The assignment variable formulated in Eq. (9). This stage ensures that each clustered user is linked to the most favorable antenna pair from a communication perspective.

$$PL_{ik}^{(\ell+1)} = PL_0 + 10n\log_{10}\left(\frac{d_{ik}^{(\ell+1)}}{d_0}\right) + X_{ik}^{\sigma} + L_{ik}^{\mathrm{2ray}} \tag{6}$$

$$P_{ikm}^{\mathrm{rx},(\ell+1)} = P_k^{\mathrm{tx}} + G_{km}^{\mathrm{tx}}(\theta_{ik}, \phi_{ik}) + G_i^{\mathrm{rx}} - PL_{ik}^{(\ell+1)} - \mathcal{A}_{ikm} \tag{7}$$

$$m_i^{*(\ell+1)} = \arg\min_{m \in \mathcal{M}_k} \mathcal{A}_{ikm} \tag{8}$$

$$y_{ikm}^{(\ell+1)} = \begin{cases} 1, & m = m_i^{*(\ell+1)} \\ 0, & \text{otherwise} \end{cases} \tag{9}$$

2.4 Interference, SINR, and Reliability Update

Once the antenna assignment is fixed, co-channel interference is estimated from neighboring clusters. It should be noted that the received powers used in the interference summation in Eq. (10) are first converted from dBm to linear milliwatt units before the SINR calculation. Therefore, if $P_{i,k,m}^{\mathrm{dBm}}$ denotes the received power from antenna sector m of cluster k, its linear value is calculated as $P_{i,k,m}^{\mathrm{lin}} = 10^{P_{i,km}^{\mathrm{dBm}}/10}$ mW. Similarly, the noise power is converted as $N_i^{\mathrm{lin}} = 10^{N_i^{\mathrm{dBm}}/10}$ mW. Thus, the interference term in Eq. (10) is evaluated using $P_{i,k,m}^{l\mathrm{lin}}$, not dBm values. In each Monte Carlo simulation trial, the sector-activity variable $s_{j,m}$ is determined from the active-user and resource-block allocation of cluster j. Specifically, $s_{j,m} = 1$ when at least one active DR user associated with sector m of neighbouring cluster j is scheduled on the same time-frequency resource block as the considered user i; otherwise, $s_{j,m} = 0$. Therefore, $s_{j,m}$ is derived from the simulated resource-block usage and is not selected as an independent arbitrary variable. The cluster-level occupancy factor ρ_j represents the fraction of time-frequency resource blocks occupied by cluster j. In the simulations, the global normalized load parameter $\rho \in [0.1, 1.0]$ controls the average cell-load condition, while ρ_j is obtained for each cluster according to its active-user density and scheduled resource-block demand. Thus, higher values of ρ

increase the probability that neighbouring sectors are active on overlapping resource blocks, which increases inter-cluster co-channel interference in Eq. (10).

$$\mathrm{I}_{\mathrm{i}}^{\mathrm{lin},(\ell+1)} = \sum_{\mathrm{j=1,j\neq k_i^*}}^{\mathrm{K}} \sum_{\mathrm{m\in M_j}} \mathrm{S}_{\mathrm{j,m}}^{(\ell+1)} \rho_{\mathrm{j}} \mathrm{P}_{\mathrm{i,j,m}}^{\mathrm{rx,\,lin},(\ell+1)} \tag{10}$$

where $\mathrm{P}_{\mathrm{i,j,m}}^{\mathrm{rx,\,lin},(\ell+1)}$ is the received interference power (mW) at user i from antenna sector m of neighbouring cluster j. The SINR is then calculated on the linear scale in Eq. (11).

$$\gamma_i^{(\ell+1)} = \frac{P_{i,k_i^*,m_i^*}^{\mathrm{lin}(\ell+1)}}{I_i^{\mathrm{lin}(\ell+1)} + N_i^{\mathrm{lin}}} \tag{11}$$

where $P_{i,k_i^*,m_i^*}^{\mathrm{lin}(\ell+1)}$ is the desired received signal power from the selected serving antenna sector, $I_i^{(\ell+1)}$ is the total neighboring-cluster interference power in milliwatts, and N_i^{lin} is the noise power in milliwatts. The obtained SINR is converted back to dB only for reporting and plotting. The achievable rate is computed in Eq. (12), and the end-to-end latency and reliability are computed in Eqs. (13) and (14), respectively. It determines whether the communication structure is suitable for real-time DR signaling in Eq. (15).

$$R_i^{(\ell+1)} = B_i \log_2\left(1 + \frac{\gamma_i^{(\ell+1)}}{\Gamma_{\mathrm{gap}}}\right) \tag{12}$$

$$\tau_i^{(\ell+1)} = \frac{L_{\mathrm{pkt}}}{R_i^{(\ell+1)}} + \tau_i^{\mathrm{queue}} + \tau_i^{\mathrm{proc}} + \tau_i^{\mathrm{prop}} + \tau_i^{\mathrm{MEC}} \tag{13}$$

$$\mathcal{R}_i^{(\ell+1)} = (1 - \mathrm{PER}_i^{(\ell+1)}) \exp(-\lambda_\tau \tau_i^{(\ell+1)}) \tag{14}$$

$$\mathrm{PER}_i^{(\ell+1)} = a_1 e^{-b_1 \gamma_i^{(\ell+1)}} \tag{15}$$

2.5 Demand Response Scheduling and Response Update

A user is considered eligible if its SINR and latency satisfy Eq. (16). For eligible users, the participation probability is calculated using the logistic response model in Eq. (17). The realized DR contribution of user i is given in Eq. (18). The aggregate demand reduction is then given in Eq. (19). This step connects the communication layer to the energy-management layer.

$$\gamma_i^{(\ell+1)} \geq \gamma_{\min},\ \tau_i^{(\ell+1)} \leq \tau_{\max} \tag{16}$$

$$q_i^{(\ell+1)}(t) = \frac{1}{1 + \exp\left[-\left(\beta_0 + \beta_1 \pi_i(t) + \beta_2 \gamma_i^{(\ell+1)} - \beta_3 \tau_i^{(\ell+1)} - \beta_4 \delta_i\right)\right]} \tag{17}$$

$$\Delta P_i^{(\ell+1)}(t) = u_i^{(\ell+1)}(t) q_i^{(\ell+1)}(t) P_i^{\max}(1 - \varepsilon_i^c(t)) \tag{18}$$

$$\Delta P_{\mathrm{DR}}^{(\ell+1)}(t) = \sum_{i=1}^{N} \Delta P_i^{(\ell+1)}(t) \tag{19}$$

2.6 Dense-Region Refinement

A cluster is considered overloaded or weak if either of the conditions given in Eq. (20) is satisfied. After this condition is satisfied, cluster k is refined. Refinement can be performed by splitting the cluster into two sub-clusters using the weighted update by Eq. (21). This refinement stage is important because it preserves communication quality in densely populated residential areas where $w_i^{(\ell+1)}$ is given as:

$$\frac{\sum_{i=1}^{N} x_{ik}^{(\ell+1)}}{\mathcal{A}_k} > \rho_{\max} \text{ OR } \min_{i:x_{ik}^{(\ell+1)}=1} \gamma_i^{(\ell+1)} < \gamma_{\text{edge}} \tag{20}$$

$$\mu_k^{(\ell+1)} = \frac{\sum_{i=1}^{N} x_{ik}^{(\ell+1)} w_i^{(\ell+1)} \mathrm{r}_i}{\sum_{i=1}^{N} x_{ik}^{(\ell+1)} w_i^{(\ell+1)}}, \text{ where } w_i^{(\ell+1)} = \frac{1}{1 + \eta_1/\gamma_i^{(\ell+1)} + \eta_2 \tau_i^{(\ell+1)} + \eta_3 \mathcal{A}_i^{(\ell+1)}} \tag{21}$$

2.7 Objective Function Evaluation and Convergence

The iterative process stops only when both the maximum centroid displacement and the relative objective variation fall below their respective thresholds, or when the maximum iteration limit is reached. At the end of iteration $l+1$, the total objective value is evaluated using normalized objective-function components. Since the objective function combines heterogeneous quantities with different physical units, each component is normalized before weighted aggregation. The normalized terms are defined as $\bar{D}^{(l+1)} = \frac{1}{N}\sum_{i=1}^{N}\sum_{k=1}^{K} x_{ik}^{(l+1)} \frac{d_{i,k}^{(l+1)}}{d_{\max}}$, $\bar{\tau}^{(l+1)} = \frac{1}{N}\sum_{i=1}^{N} \frac{\tau_i^{(l+1)}}{\tau_{\max}}$, $\bar{U}^{(l+1)} = \frac{1}{N}\sum_{i=1}^{N}\left(1 - \mathcal{R}_i^{(l+1)}\right)$, $\bar{A}^{(l+1)} = \frac{1}{N}\sum_{i=1}^{N} \frac{A_{i,k,m}^{(l+1)}}{A_{\max}}$, $\bar{G}_{DR}^{(l+1)}(t) = \frac{\Delta P_{DR}^{(l+1)}(t)}{P_{\max}}$, $\bar{C}_{risk}^{(l+1)}(t) = \frac{CVaR_\eta\left(S^{(l+1)}(t)\right)}{S_{\max}}$ where $d_{\max}$, $\tau_{\max}$, $A_{\max}$, $P_{\max}$, and $S_{\max}$ are the reference scaling values for distance, latency, attenuation, maximum DR capacity, and shortage-risk normalization, respectively. The normalized objective function is then written in Eq. (22):

$$J^{(l+1)} = \sum_{t=1}^{T}\left[\alpha_1 \bar{D}^{(l+1)} + \alpha_2 \bar{\tau}^{(l+1)} + \alpha_3 \bar{U}^{(l+1)} + \alpha_4 \bar{A}^{(l+1)} - \alpha_5 \bar{G}_{DR}^{(l+1)}(t) + \alpha_6 \bar{C}_{risk}^{(l+1)}(t)\right] \tag{22}$$

The DR gain term is subtracted because higher controllable DR response is desirable, whereas the remaining terms are minimized. This normalized formulation ensures that no objective component dominates due to its physical scale. The iterative process stops only when both the maximum centroid displacement and the relative objective variation fall below their respective thresholds, or when the maximum iteration limit is reached as Eq. (23):

$$\max_k \parallel \mu_k^{(l+1)} - \mu_k^{(l)} \parallel_2 \le \varepsilon_\mu \text{ and } \Delta J_{rel}^{(l)} = \frac{\mid J^{(l+1)} - J^{(l)} \mid}{J^{(l)}} \le \varepsilon_J, \text{or } l = l_{\max} \tag{23}$$

The weighting factors in Table 2 were selected using a heuristic tuning approach guided by the design priorities of the proposed CCA-DR framework. Since the main objective is to improve controllable DR participation while maintaining reliable 5G communication, the highest weight was assigned to the DR gain term $(\alpha_5 = 0.30)$. The distance component $(\alpha_1 = 0.20)$ supports compact and balanced clustering, while latency and unreliability $(\alpha_2 = \alpha_3 = 0.15)$ reflect the importance of real-time and reliable DR signalling. Attenuation and CVaR shortage risk $(\alpha_4 = \alpha_6 = 0.10)$ were assigned smaller but non-zero weights to include link quality.

The results were not found to be sensitive to the choice of a single manual weight setting and a short sensitivity analysis is examined at $\rho = 0.5$. For the communication-priority setting, higher weights were given to latency, unreliability, attenuation and compactness; and lower weight was given to DR-gain as shown in Table 3. With DR-priority set, the DR-gain weight was raised and the other weights were adjusted accordingly. The results demonstrate the stability of the proposed CCA-DR framework under the tested settings. The DR-gain weight can be increased to gain aggregate DR response but at the cost of modest increase in latency and a small decrease in reliability, while the communication-priority weighting can be increased to gain latency and reliability at the cost of a modest decrease in aggregate DR response. This reaffirms that the chosen baseline weights represent a consistent balance between communication quality, DR response, reliability and fairness.

Table 2: Objective-function components, normalization terms, and weighting factors used in the proposed model.

Component	Normalization	Weight	Purpose
Distance	$d_{i,k}/d_{max}$	0.20	Reduce cluster spread
Latency	τ_i/τ_{max}	0.15	Maintain real-time DR signalling
Unreliability	$1-\mathcal{R}_i$	0.15	Improve delivery reliability
Attenuation	$A_{i,k,m}/A_{max}$	0.10	Prefer stronger antenna links
DR gain	$\Delta P_i/P_{max}$	0.30	Increase controllable DR response
CVaR shortage risk	$CVaR\eta(S)/S_{max}$	0.10	Penalize the shortage risk

Table 3: Sensitivity analysis of CCA-DR performance to objective-function weights setting.

Setting	α_1	α_2	α_3	α_4	α_5	α_6	Lat.	DR	Rel.	JFI
Comm-priority	0.22	0.18	0.18	0.12	0.20	0.10	6.55	512.4	0.72	0.83
Baseline	0.20	0.15	0.15	0.10	0.30	0.10	6.80	536.7	0.70	0.82
DR-priority	0.18	0.13	0.13	0.09	0.37	0.10	7.15	558.2	0.68	0.80

Note: Lat. = latency (ms); DR = aggregate demand response (kW); Rel. = reliability; JFI = Jain fairness index.

3 Iterative Communication-Aware Clustered DR Management under 5G

Input: User coordinates $\{r_i\}$, number of clusters K, antenna set M_k, transmit power, channel parameters, QoS thresholds, DR parameters, convergence tolerances ε_μ and ε_J, maximum iterations $L_{\max}$

Output: Final cluster assignments x_{ik}, centroids μ_k, antenna assignments y_{ikm}, SINR γ_i, delay τ_i, reliability $\mathcal{R}_i$, aggregate DR response ΔP_{DR}, whereas (see Algorithm 1):

Algorithm 1: Iterative communication-aware clustered DR management

Initialize iteration counter $\ell = 0$
Initialize cluster centroids $\mu_k^{(0)}$
Set the previous objective $J^{(0)} = +\infty$
repeat
for each user $i = 1$ to N **do**
Compute distance $d_{ik}^{(\ell)}$ to each centroid k
Compute communication-aware clustering cost $C_{ik}^{(\ell)}$
Assign user i to the minimum-cost cluster
Update $x_{ik}^{(\ell+1)}$
end for
Enforce cluster size constraints and rebalance if needed
for each assigned user i **do**
Compute path loss $PL_{ik}^{(\ell+1)}$
for each candidate antenna pair $m \in M_k$ **do**
Compute received power $P_{rx,ikm}^{(\ell+1)}$

(Continued)

Algorithm 1 (continued)

16: Compute cumulative attenuation A_{ikm}
17: end for
18: Select antenna pair m_i^* with minimum attenuation
19: Update $y_{ikm}^{(\ell+1)}$
20: end for
21: for each active user $\boldsymbol{i}$ **do**
22: Compute interference $I_i^{(\ell+1)}$
23: Compute SINR $\gamma_i^{(\ell+1)}$
24: Compute data rate $R_i^{(\ell+1)}$
25: Compute latency $\tau_i^{(\ell+1)}$
26: Compute the packet error rate $PER_i^{(\ell+1)}$
27: Compute reliability $\mathcal{R}_i^{(\ell+1)}$
28: end for
29: for each user $\boldsymbol{i}$ **do**
30: Compute the participation probability $q_i^{(\ell+1)}$
31: Determine DR activation $u_i^{(\ell+1)}$
32: Compute realized demand reduction $\Delta P_i^{(\ell+1)}$
33: end for
34: Compute $\Delta P_{DR}^{(\ell+1)} = \sum_i \Delta P_i^{(\ell+1)}$
35: for each cluster k **do**
36: Check density threshold and edge-SINR threshold
37: if violated, then refine or split cluster k
38: Update centroid $\mu_k^{(\ell+1)}$ using the weighted rule
39: end for
40: Evaluate objective $J^{(\ell+1)}$
41: Until $\max\limits_k \parallel \mu_k^{(l+1)} - \mu_k^{(l)} \parallel_2 \leq \varepsilon_\mu$ **and** $\frac{|J^{(l+1)} - J^{(l)}|}{J^{(l)}} \leq \varepsilon_J$, **or** $l = l_{\max}$
42: Return $x_{ik}, \mu_k, y_{ikm}, \gamma_i, \tau_i, \mathcal{R}_i, \Delta P_{DR}$

3.1 Simulation Configuration and Reproducibility Protocol

The simulation was made reproducible using a fixed master random seed, rng(7). The master random seed rng(7) was used only once to initialize the pseudo-random number generator. For each Monte Carlo trial, a unique trial-specific seed was deterministically generated from the master random sequence, thereby producing an independent realization of user locations, shadow fading, channel conditions, and traffic demand. To ensure a fair comparison, the same trial realization was used for all competing schemes, including the proposed CCA-DR, Distance-Only clustering, Greedy Antenna selection, Static Clustering, and Unicast DR. Each algorithm therefore operated on identical network conditions within a given trial, and only the optimization strategy differed. After all algorithms completed the same realization, the next trial-specific seed was used to generate a new independent realization. Consequently, the reported performance metrics represent averages over 100 independent but fully reproducible Monte Carlo trials. The mean value, the standard deviation and the 95% confidence interval were then calculated based on 100 independent but reproducible simulation realizations. A 2000 × 2000 m^2 5G-enabled smart-grid service area was considered, with 500 uniformly distributed DR users unless otherwise stated. By default, 9 clusters were considered, each with 4 directional antenna sectors that are uniformly spaced at 0°, 90°, 180°, and 270°. The half-power beamwidth of the antenna was 65° and the directionality attenuation was determined by calculating an angle between the user and the selected sector. The wireless channel was modeled as a path-loss model with log-normal shadowing with the path-loss constant PL_0 = 32.4 dB at d_0 = 1 m and the path-loss exponent n = 3.1, and the standard deviation of shadowing σ = 6 dB. The transmit power of the small-cells was 30 dBm and the transmitter and the receiver's antennae gains were 9 and 2 dBi, respectively. The implementation gap Γgap was 1.5, the bandwidth of the system was 100 MHz and the thermal noise density was −174 dBm/Hz. To evaluate the effects of light-load to full-load conditions, the normalized cell-load factor ρ varied from 0.1 to 1.0 with a step of 0.1, with ρ = 0 being omitted as it represents an idle network with no active DR signalling, queueing delay, or meaningful cell loss.

4 Results and Discussion

For a fair comparison, the proposed CCA-DR framework is compared with four benchmark schemes in the same user distribution, channel model, antenna configuration, load range, Monte Carlo trials, QoS thresholds and performance metrics. Distance-Only clustering assigns users to the closest centroid based on the Euclidean distance only, and does not take any other factors into account, such as path loss, SINR, latency, reliability, or antenna attenuation. Greedy Antenna selection, selects the locally strongest or least attenuated one without joint clustering or iterative refinement. Static Clustering maintains the existing user-cluster mapping in spite of changes in load or communication quality. Unicast DR does NOT do clustered communication and/or does NOT optimize directionally at the cluster level, only one-to-one.

4.1 Load-Dependent Communication Performance Analysis

Fig. 1a shows that average latency increases with normalized cell load ρ due to higher interference, scheduling pressure, and queuing delay. However, the proposed framework of CCA-DR is able to achieve the lowest latency for all load conditions, from approximately 5 ms for ρ = 0.1 up to almost 13 ms for ρ = 1.0, all of which are still below the 20 ms real-time DR requirement. Distance-Only and Greedy Antenna schemes achieve times around 14–15 ms, while Static Clustering gets to 16–17 ms, and Unicast DR jumps considerably to 26 ms, reflecting a poor scalability of one-to-one DR signalling. The same trend is also seen on the graph of packet loss in Fig. 1b. At full load, the packet loss of CCA-DR is the lowest (around 0.04), while Distance-Only, Greedy Antenna and Static Clustering packet loss is around 0.09–0.14, and Unicast DR is around 0.55–0.56. This improvement is attributed as a result of compact clustering, directional antenna assignment, and iterative refinement to decrease the weak links and congested communication regions. The further confirmation of the CCA-DR communication advantage is shown in Fig. 1c. In the case of higher load, SINR of all the schemes reduces, however, SINR of CCA-DR decreases the least which is from approximately 32 dB to 22–23 dB at full load. Compared to that, Distance-Only drops down to around 19 dB, Greedy Antenna to 18 dB, Static Clustering to 16–17 dB and Unicast DR only to 6–7 dB. This shows that CCA-DR considers both spatial association and communication quality. The user-rate results in Fig. 2a also support this finding. CCA-DR decreases from about 2.5 Mbps at low load to 1.7–1.8 Mbps at high load, still outperforming the benchmark schemes. Fig. 2b shows that CCA-DR maintains the highest active DR user ratio, remaining near 1.0 under light load and about 0.92 under heavy load, while the benchmark schemes remain much lower. Finally, Fig. 2c shows that reliability decreases with increasing load, but CCA-DR remains the most reliable, declining from about 0.78 to 0.55, compared with only 0.17–0.18 for Unicast DR. Overall, the proposed framework enhances the DR communication performance by lowering latency, packet loss, and increasing SINR, user rate, active-user ratio and reliability, compared with the performance of the Unicast DR approach.

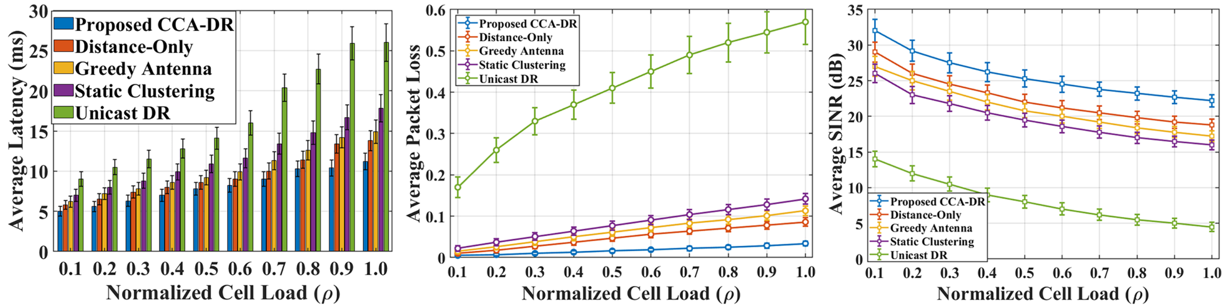

(a) (b) (c)

Figure 1: Performance comparison of the proposed CCA-DR framework and benchmark schemes under varying normalized cell load: (**a**) average network latency; (**b**) average packet loss; and (**c**) average SINR. Bars/markers represent mean values over 100 independent Monte Carlo trials, and error bars indicate 95% confidence intervals computed separately for each method and load point.

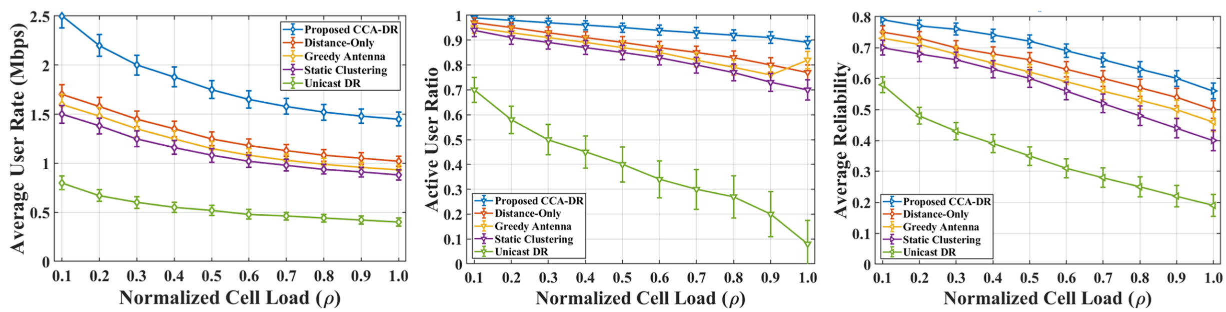

(a) (b) (c)

Figure 2: Performance comparison of the proposed CCA-DR framework and benchmark schemes under varying normalized cell load: (**a**) average user rate; (**b**) active DR user ratio; and (**c**) average communication reliability. Markers represent mean values over 100 independent Monte Carlo trials, and error bars indicate 95% confidence intervals computed separately for each method and load point.

4.2 Fairness, Edge-User Robustness, and CDF-Based Validation

The CDF plots are reported at $\rho = 0.5$ to represent a balanced medium-load condition, while the full load-dependent evaluation is performed over $\rho = 0.1$ to $\rho = 1.0$. Fig. 3a shows that the proposed CCA-DR framework maintains a high Jain fairness index, decreasing only from about 0.84 at light load to about 0.78 at full load. In contrast, the benchmark schemes show greater degradation, with Unicast DR approaching 0.05. This confirms that CCA-DR avoids consistently favoring users with strong links and improves fairness by refining clusters and supporting users in poor communication regions. The 10th percentile cell-edge SINR in Fig. 3b further confirms edge-user robustness. CCA-DR decreases from about 19 dB to 9–10 dB at maximum load, whereas the benchmark schemes suffer larger reductions, and Unicast DR becomes negative at full load. This shows that CCA-DR improves both average performance and cell-edge reliability. User-level validation at $\rho = 0.5$ is shown through the CDF results. The latency CDF in Fig. 3c shifts farthest to the left, indicating lower and more consistent latency. Similarly, the packet-loss CDF in Fig. 4a rises sharply in the low-loss region, showing that most users experience limited packet loss. The SINR and user-rate CDFs in Fig. 4b,c also show that more users achieve higher SINR and better data rates under the proposed method.

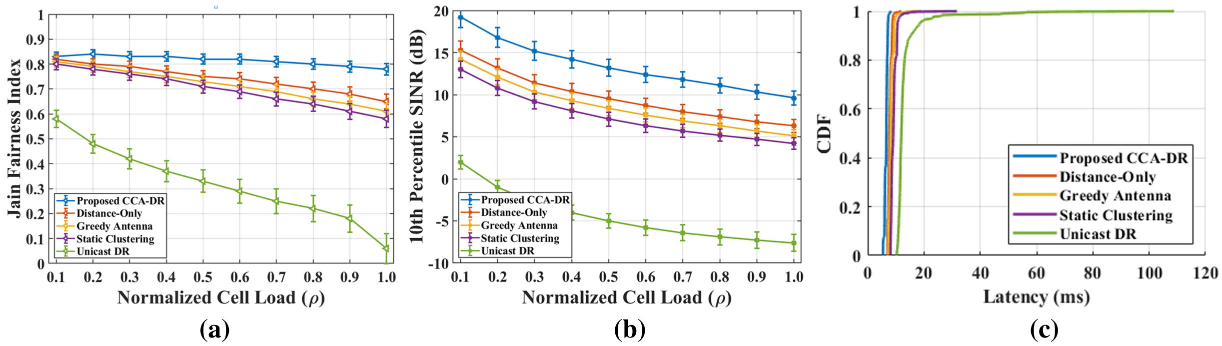

Figure 3: Fairness, cell-edge, and distributional performance of the proposed CCA-DR framework and benchmark schemes: (**a**) Jain fairness index under varying normalized cell load; (**b**) 10th percentile cell-edge SINR under varying normalized cell load; and (**c**) latency CDF at $\rho = 0.5$. Error bars in Fig. 3a,b indicate 95% confidence intervals computed over 100 independent Monte Carlo trials.

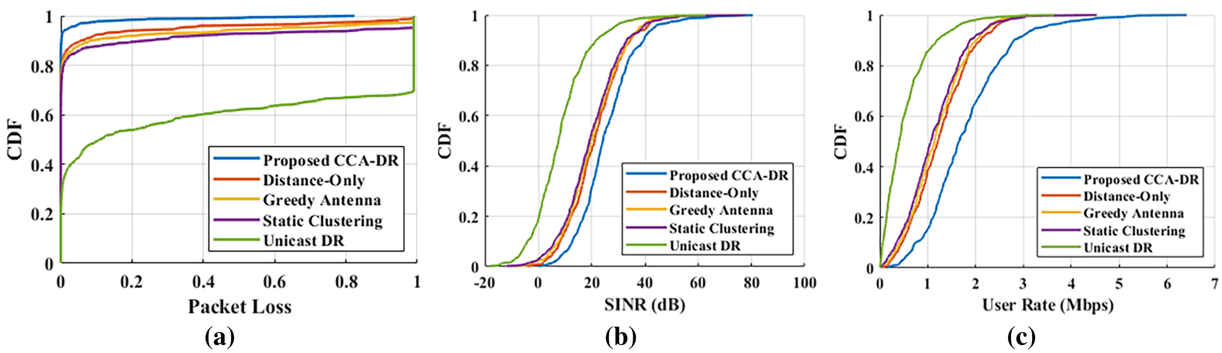

Figure 4: Distributional performance of the proposed CCA-DR framework and benchmark schemes: (**a**) Packet-loss CDF at $\rho = 0.5$; (**b**) SINR CDF at $\rho = 0.5$; and (**c**) User-rate CDF at $\rho = 0.5$.

4.3 Reliability, Runtime, Incentive, and Cluster Sensitivity Analysis

Fig. 5a shows that CCA-DR has the most favourable reliability CDF, confirming that the improvement is distributed across users rather than limited to average performance. The directional antenna layout and spatial cluster map in Fig. 5b further illustrate how users are assigned to smaller service areas, while directional sectors reduce transmission distance, attenuation, packet loss, and cell-edge degradation. Fig. 5c shows that CCA-DR has higher runtime than Greedy Antenna and Unicast DR because it includes clustering, channel evaluation, antenna assignment, and iterative refinement; however, the runtime remains practical, reaching about 13 ms for 500 users. Fig. 6a shows that CCA-DR achieves a higher aggregate DR response across all incentive levels, while Fig. 6b indicates that reliability is less affected by incentives because it mainly depends on channel quality, packet loss, latency, and interference. Finally, Fig. 6c confirms that the number of clusters is an important design parameter, where a moderate cluster setting provides the best balance between DR response and communication quality.

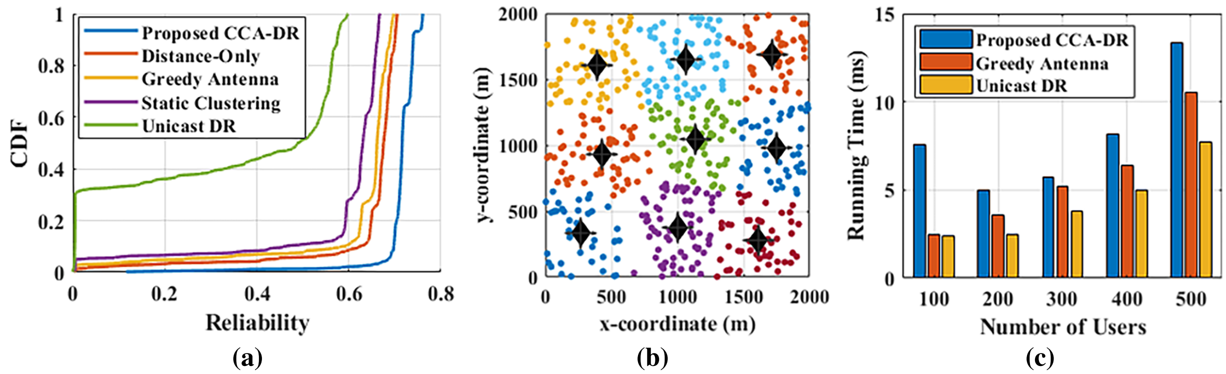

Figure 5: Reliability distribution, spatial layout, computational complexity, and sensitivity analysis of the proposed CCA-DR framework: (**a**) Communication reliability CDF at the representative medium-load condition ρ = 0.5; (**b**) Spatial cluster map with directional antenna layout; (**c**) Algorithmic running time vs. network size.

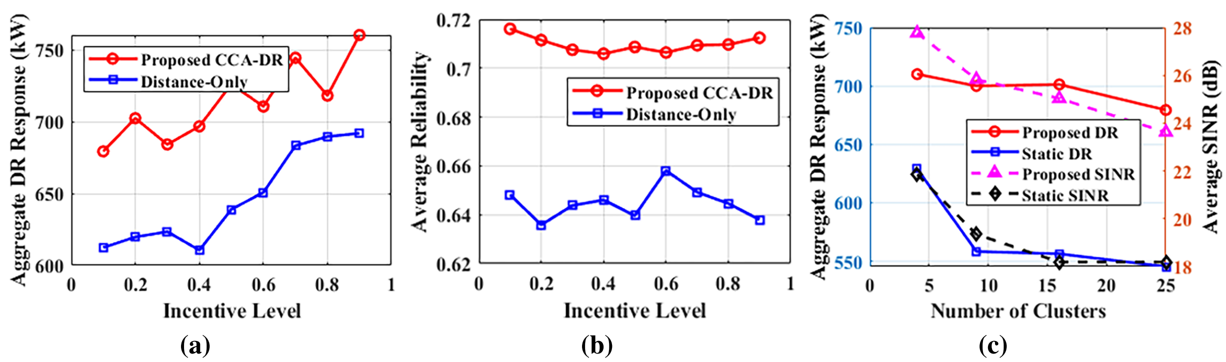

Figure 6: Sensitivity analysis of the proposed CCA-DR framework: (**a**) Effect of incentive level on aggregate DR response; (**b**) Effect of incentive level on average communication reliability; and (**c**) Sensitivity of aggregate DR response and average SINR to the number of clusters.

4.4 Convergence and Ablation-Based Performance Validation

All major simulations were repeated over N_{MC} = 100 independent Monte Carlo trials. Each algorithm has been tested 100 times and each normalized cell-load point has been tested for each algorithm, and the reported value is the mean of the samples. The statistical uncertainty was evaluated by computing the 95% confidence interval, $CI_{95} = 1.96\frac{\sigma}{\sqrt{N_{MC}}}$ where σ is taken as the sample standard deviation over the Monte Carlo trials. Each of the methods, metrics, and load points have their own separate 95% confidence interval. The resulting 95% confidence intervals are displayed as error bars in Figs. 1a–c, 2a–c and 3a,b. The relatively small confidence intervals for the primary performance measures suggest that the improvements that were measured in CCA-DR are not attributable to just one random network realization and are consistent across the independent Monte Carlo trials.

The convergence behaviour of the proposed iterative CCA-DR algorithm is illustrated in Fig. 7 under the representative medium-load condition ρ = 0.5, with N = 500 users, K = 9 clusters, M_k = 4 antenna sectors per cluster, and N_{MC} = 100 independent Monte Carlo trials. Fig. 7a shows the normalized objective-function value $J^{(l)}$, which decreases rapidly during the initial iterations before gradually converging to a stable value. Fig. 7b presents the centroid movement $\Delta\mu^{(l)}$, demonstrating that the centroid displacement decreases monotonically and falls below the centroid tolerance $\varepsilon_{\mu} = 10^{-3}$ m. Fig. 7c illustrates the relative objective variation, $\Delta J_{\mathrm{rel}}^{(l)} = \frac{|J^{(l+1)} - J^{(l)}|}{J^{(l)}}$, together with the objective-function tolerance $\varepsilon_J = 10^{-4}$. The vertical dashed line indicates the actual stopping iteration, at which both convergence criteria are satisfied simultaneously. These results confirm that the proposed CCA-DR algorithm converges efficiently within a limited number of iterations while satisfying both the centroid-based and objective-based stopping conditions. The stopping iteration shown in Fig. 7 corresponds to the first iteration at which both the centroid-movement criterion and the relative objective-variation criterion are simultaneously satisfied as per Eq. (23).

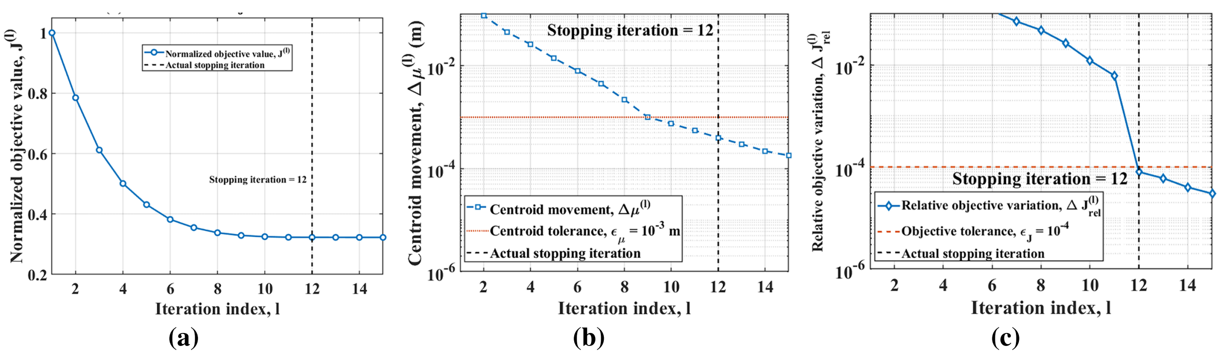

Figure 7: Convergence behaviour of the proposed CCA-DR algorithm under $\rho = 0.5$, $J^{(l)}$, $\Delta\mu^{(l)}$, $\varepsilon_\mu = 10^{-3}$ m, $\Delta J_{\mathrm{rel}}^{(l)}$, and $\varepsilon_J = 10^{-4}$: (**a**) normalized objective-function value $J^{(l)}$; (**b**) centroid movement $\Delta\mu^{(l)}$ with centroid tolerance $\varepsilon_\mu = 10^{-3}$ m; (**c**) relative objective variation $\Delta J_{\mathrm{rel}}^{(l)} = | J^{(l+1)} - J^{(l)} | / J^{(l)}$ with objective tolerance $\varepsilon_J = 10^{-4}$. The vertical dashed line denotes the actual stopping iteration where both criteria are satisfied.

The ablation study in Table 4 distinguishes the effect of each major components of the proposed framework: communication-aware clustering, direction-specific assignment of antennas, and iterative refinement. All three are not included in the Distance-Only baseline. The second variant is a communication-aware clustering only. The third—Directional Antenna Assignment—does not include iterative refinement. All three components are part of the complete CCA-DR framework. The results are given as mean ± 95% confidence interval based on 100 independent Monte Carlo trials at $\rho = 0.5$. This presentation shows both the incremental contribution of each component and the statistical robustness of the observed performance differences.

Table 4: Compact ablation study of the proposed CCA-DR framework at $\rho = 0.5$.

Variant	CAC	DAA	IR	Lat. (ms)	PL	SINR (dB)	Rate	ADR	Rel.	JFI
Distance-Only	No	No	No	8.30 ± 0.18	0.050 ± 0.004	22.0 ± 0.7	1.35 ± 0.05	0.90 ± 0.02	0.63 ± 0.02	0.78 ± 0.02
CCA-DR w/o DAA	Yes	No	No	7.70 ± 0.15	0.038 ± 0.003	23.5 ± 0.6	1.55 ± 0.04	0.93 ± 0.02	0.66 ± 0.02	0.80 ± 0.02
CCA-DR w/o IR	Yes	Yes	No	7.20 ± 0.13	0.029 ± 0.003	24.5 ± 0.5	1.75 ± 0.04	0.96 ± 0.01	0.68 ± 0.02	0.81 ± 0.01
Full CCA-DR	Yes	Yes	Yes	6.80 ± 0.12	0.021 ± 0.002	25.2 ± 0.5	1.90 ± 0.03	0.98 ± 0.01	0.70 ± 0.01	0.82 ± 0.01

Note: CAC = communication-aware clustering; DAA = directional antenna assignment; IR = iterative refinement; PL = packet loss; ADR = active DR ratio; Rel. = reliability; JFI = Jain fairness index. Values are reported as mean ± 95% ($CI_{95} = 1.96\frac{\sigma}{\sqrt{100}}$) confidence interval over 100 independent Monte Carlo trials at $\rho = 0.5$.

4.5 Comparative Analysis with Existing DR and 5G Communication Studies

A comparison in Table 5 shows that the studies available typically address only one aspect of the problem. For instance, Ref. [11] addresses dynamic pricing for DR, Ref. [12] addresses latency-aware DR for wireless networks, Ref. [13] addresses real-time user-side energy management for DR, and Ref. [15] discusses the challenges in DR communication in IoT. However, these studies cannot be combined to assess dense 5G communication metrics, including packet loss, cell-edge performance, SINR, antenna assignment, active DR user ratio, and fairness. Although some recent studies report useful communication metrics for LPWAN smart-grid communication [17], 5G dual-connectivity handover [18], and QoS-aware 5G MTC scheduling [19], they do not jointly address DR activation, clustered 5G coordination, directional antenna assignment, and communication-aware DR management. Unlike the proposed CCA-DR framework, it offers a DR-aware and communication-aware evaluation. It is tested under normalized cell load from $\rho = 0.1$ to $\rho = 1.0$ and jointly measures latency, packet loss, SINR, user rate, active DR user ratio, reliability, fairness, and cell-edge SINR. The proposed model maintains latency around 5–13 ms, which remains below the 20 ms DR threshold, and keeps packet loss around 0.04 at full load. It also achieves an SINR of 22–23 dB, an active DR ratio of 0.92, fairness of 0.78, and a cell-edge SINR of 9–10 dB at full load.

Table 5: Positioning of the proposed CCA-DR framework against related DR and communication-aware studies.

Ref.	Study Focus	Key Comparison
[11]	DR dynamic pricing with multi-agent reinforcement learning	DR optimization focused; no 5G SINR, packet loss, or cell-edge evaluation.
[12]	Latency-aware DR in distributed wireless networks	Considers DR latency, but not 5G clustered antenna-based coordination.
[13]	Edge-based user-side energy management	Supports real-time DR, but does not evaluate dense 5G DR signalling.
[15]	IoT-enabled smart-grid DR	Discusses DR communication issues, but not 5G clustering or antenna assignment.
[17]	Hybrid LPWAN smart-grid communication	Packet delivery >97%; SNR ≈ 9 dB; latency <150 ms; reliability = 0.98.
[18]	5G dual-connectivity handover	>95% lower interruption time; 10× lower failure; packet delivery = 99.9%.
[19]	QoS-aware 5G MTC scheduling	Fairness ≈ 0.78; delay violation capped at 8.3; throughput ≈ 15% below Best-CQI.
Proposed CCA-DR	5G clustered communication-aware DR	$\rho = 0.1$ to $\rho = 1.0$; latency ≈ 5–13 ms; packet loss ≈ 0.04; SINR ≈ 22–23 dB; active DR ratio ≈ 0.92; fairness ≈ 0.78.

5 Practical Deployment Implications

To begin with, the proposed framework's ability to keep latency low even under heavy normalized cell loading demonstrates its applicability to near-real-time DR dispatch, where control delays can make load adjustments less effective. Second, fairness and cell-edge SINR are improved, indicating that the scheme is more applicable to large-scale residential deployments, as it reduces the likelihood that users in poor communication areas are repeatedly locked out of DR participation. Third, the small runtime cost across the largest network sizes considered, suggests that the method is computationally efficient to execute with the assistance of edges. Lastly, the cluster-count sensitivity analysis indicates that a fixed clustering assumption cannot be relied upon for practical deployment; cluster granularity needs to be adjusted based on user density, interference, and the properties of the service area to achieve an optimal compromise between communication quality and DR responsiveness.

6 Conclusion and Future Work

This paper proposes a communication-aware clustered demand response (CCA-DR) framework in the smart grid with 5G technology. The proposed solution overcomes major disadvantages of the existing DR solutions in dense networks where latency, packet loss, low signal strength, and lack of connectivity with users can decrease the effectiveness of the DR. The study combines DR user clustering, nearest-centroid association, 5G channel modelling, directional antenna pair selection, and dense-region refinement into an iterative procedure and considers DR management as an energy-management and communication-constrained optimization problem. For all four benchmark schemes, Distance-Only clustering, Greedy Antenna selection, Static Clustering, and Unicast DR, the proposed CCA-DR framework is shown to outperform the others in terms of both latency and packet-loss, SINR and user rate, the ratio of active DR users, reliability, fairness, and cell-edge robustness as the normalized cell load increases. Further, CDF-based results validate the proposed scheme to provide more stable and predictable latency, packet loss, and reliability performance across users. Based on runtime analysis, the framework is seen to be still computationally feasible, and the incentive and cluster-sensitivity results confirm that moderate clustering offers the best trade-off between DR response and communication quality. In conclusion, the results show that the 5G communication awareness in clustering, association, and antenna assignment can significantly enhance the efficiency, reliability, fairness, and scalability of DR management in future smart-grid systems.

The framework can be extended in future work to include additional, more realistic communication conditions, including handover events, MEC failures, and dynamic traffic loads. Secure signalling delay, attack-resilience overhead, and other cybersecurity-aware metrics can also be included in the DR optimization model. In addition, adaptive cluster formation depending on the number of users and renewable energy integration can further help enhance the resilience of 5G-enabled DR management in the future smart grid.

Acknowledgement: Princess Nourah bint Abdulrahman University Researchers Supporting Project number (PNURSP2026R140), Princess Nourah bint Abdulrahman University, Riyadh, Saudi Arabia.

Funding Statement: Princess Nourah bint Abdulrahman University Researchers Supporting Project number (PNURSP2026R140), Princess Nourah bint Abdulrahman University, Riyadh, Saudi Arabia.

Author Contributions: The authors confirm contribution to the paper as follows: conceptualization, Sajjad Rabbani; methodology, Sajjad Rabbani; validation, Adnan Yousaf, Rao Muhammad Asif; formal analysis, Adnan Yousaf, Ateeq Ur Rehman; investigation, Sajjad Rabbani, Rao Muhammad Asif; resources, Heba G. Mohamed, Ateeq Ur Rehman; data curation, Sajjad Rabbani; writing—original draft preparation, Sajjad Rabbani, Heba G. Mohamed; writing—review and editing, Adnan Yousaf, Ateeq Ur Rehman; supervision, Rao Muhammad Asif, Adnan Yousaf; funding acquisition, Heba G. Mohamed. All authors reviewed and approved the final version of the manuscript.

Availability of Data and Materials: Not applicable.

Ethics Approval: Not applicable.

Conflicts of Interest: The authors declare no conflicts of interest.

References

1. Hui H, Ding Y, Shi Q, Li F, Song Y, Yan J. 5G network-based Internet of Things for demand response in smart grid: a survey on application potential. Appl Energy. 2020;257(5):113972. doi:10.1016/j.apenergy.2019.113972.
2. Dev A, Kumar V, Khare G, Giri J, Amir M, Ahmad F, et al. Advancements and challenges in microgrid technology: a comprehensive review of control strategies, emerging technologies, and future directions. Energy Sci Eng. 2025;13(4):2112–34. doi:10.1002/ese3.2095.
3. Powell J, McCafferty-Leroux A, Hilal W, Gadsden SA. Smart grids: a comprehensive survey of challenges, industry applications, and future trends. Energy Rep. 2024;11(23):5760–85. doi:10.1016/j.egyr.2024.05.051.
4. Ali A, Koucheryavy Y. Adaptive beam tracking in 5G/6G mmWave networks: a clustered federated learning approach. IEEE Access. 2025;13(5):70705–20. doi:10.1109/ACCESS.2025.3563435.
5. Firouzi R, Rahmani R. Delay-sensitive resource allocation for IoT systems in 5G O-RAN networks. Internet Things. 2024;26(6):101131. doi:10.1016/j.iot.2024.101131.
6. Ichkov A, Wietfeld A, Petrova M, Simić L. HBF MU-MIMO with interference-aware beam pair link allocation for beyond-5G mm-wave networks. IEEE Trans Mob Comput. 2025;24(5):4248–62. doi:10.1109/TMC.2025.3526547.
7. Verdecia-Peña R, Muriel-Barrado AT, Calatayud-Maeso J, Sanchez-Olivares P, Fernández-González JM, Alonso JI. A millimeter-wave phased array-aided 5G communication prototype: evaluation in an indoor scenario. IEEE Access. 2024;12:155804–20. doi:10.1109/ACCESS.2024.3483573.
8. Lu H, Xia W, Miao W, Zhang M, Yan F, Shen L. Resource allocation in user-centric cell-free massive MIMO URLLC systems with network slicing. IEEE Access. 2025;13:130215–31. doi:10.1109/ACCESS.2025.3591008.
9. Yousaf A, Asif RM, Shakir M, Rehman AU, Adrees MS. An improved residential electricity load forecasting using a machine-learning-based feature selection approach and a proposed integration strategy. Sustainability. 2021;13(11):6199. doi:10.3390/su13116199.
10. Ahmed F, Arshad A, Rehman AU, Hussain GA, Lehtonen M. A multi-agent reinforcement learning framework for voltage-constrained incentive demand response in PV-rich low-voltage distribution systems. IEEE Access. 2026;14:45410–22. doi:10.1109/ACCESS.2026.3674153.
11. Ma H, Zhang H, Tian D, Yue D, Hancke GP. Optimal demand response based dynamic pricing strategy via multi-agent federated twin delayed deep deterministic policy gradient algorithm. Eng Appl Artif Intell. 2024;133(4):108012. doi:10.1016/j.engappai.2024.108012.
12. Ding Q, Liu Q, Shi H, Luo J. Demand response management with latency difference in distributed wireless network. CSEE J Power Energy Syst. 2025;11(3):1312–21. doi:10.17775/CSEEJPES.2022.07590.
13. Huang J, Zhou S, Li G, Shen Q. Real-time monitoring and optimization methods for user-side energy management based on edge computing. Sci Rep. 2025;15(1):24890. doi:10.1038/s41598-025-07592-4.
14. Cheng Z, Li J, Zhang J, Wang C, Wang H, Wu J. Application of edge computing technology in smart grid data security. Meas Sens. 2025;37(6):101412. doi:10.1016/j.measen.2024.101412.
15. Ma L, Hui H, Wang S, Song Y. Coordinated optimization of power-communication coupling networks for dispatching large-scale flexible loads to provide operating reserve. Appl Energy. 2024;359:122705. doi:10.1016/j.apenergy.2024.122705.
16. Arévalo P, Jurado F. Impact of artificial intelligence on the planning and operation of distributed energy systems in smart grids. Energies. 2024;17(17):1–22. doi:10.3390/en17174501.
17. Veloso AFS, Reis JV Jr, Rabelo RAL. A microservices-based solution with hybrid communication for energy management in smart grid environments. Sensors. 2026;26(5):1714. doi:10.3390/s26051714.
18. Hamarsheh A, El-Taj HRK, Al-Qerem A, Alauthman M. Optimizing handover performance in 5G networks using dual connectivity. Wirel Pers Commun. 2026;146(4):1923–87. doi:10.1007/s11277-026-11944-2.
19. Khunteta A, Baheti PK. QoS-aware resource scheduling for machine type communication in 5G networks. J King Saud Univ. 2026;38(4):33. doi:10.1007/s44444-026-00107-0.